

# Non-Invasive Pressure Reactivity Index Using Doppler Systolic Flow Parameters: A Pilot Analysis

Frederick A. Zeiler,<sup>1-3</sup> Peter Smielewski,<sup>4</sup> Andrew Stevens,<sup>1</sup> Marek Czosnyka,<sup>4,5</sup>  
David K. Menon,<sup>1</sup> and Ari Ercole<sup>1</sup>

## Abstract

The goal was to predict pressure reactivity index (PRx) using non-invasive transcranial Doppler (TCD) based indices of cerebrovascular reactivity, systolic flow index (Sx\_a), and mean flow index (Mx\_a). Continuous extended duration time series recordings of middle cerebral artery cerebral blood flow velocity (CBFV) were obtained using robotic TCD in parallel with direct intracranial pressure (ICP). PRx, Sx\_a, and Mx\_a were derived from high frequency archived signals. Using time-series techniques, autoregressive integrative moving average (ARIMA) structure of PRx was determined and embedded in the following linear mixed effects (LME) models of PRx:  $PRx \sim Sx\_a$  and  $PRx \sim Sx\_a + Mx\_a$ . Using 80% of the recorded patient data, the LME models were created and trained. Model superiority was assessed via Akaike information criterion (AIC), Bayesian information criterion (BIC), and log-likelihood (LL). The superior two models were then used to predict PRx using the remaining 20% of the signal data. Predicted and observed PRx were compared via Pearson correlation, linear models, and Bland–Altman (BA) analysis. Ten patients had 3–4 h of continuous uninterrupted ICP and TCD data and were used for this pilot analysis. Optimal ARIMA structure for PRx was determined to be (2,0,2), and this was embedded in all LME models. The top two LME models of PRx were determined to be:  $PRx \sim Sx\_a$  and  $PRx \sim Sx\_a + Mx\_a$ . Estimated and observed PRx values from both models were strongly correlated ( $r > 0.9$ ;  $p < 0.0001$  for both), with acceptable agreement on BA analysis. Predicted PRx using these two models was also moderately correlated with observed PRx, with acceptable agreement ( $r = 0.797$ ,  $p = 0.006$ ;  $r = 0.763$ ,  $p = 0.011$ ; respectively). With application of ARIMA and LME modeling, it is possible to predict PRx using non-invasive TCD measures. These are the first and as well as being preliminary attempts at doing so. Much further work is required.

**Keywords:** autoregulation; brain injury; TBI; TCD; time series

## Introduction

**P**RESSURE REACTIVITY INDEX (PRx) is considered the “gold standard” of continuous cerebrovascular reactivity monitoring after traumatic brain injury (TBI).<sup>1,2</sup> Derived from the moving correlation coefficient between slow-wave fluctuations in intracranial pressure (ICP) and mean arterial pressure (MAP), PRx provides a continuously updating assessments of cerebral autoregulation, with positive values indicative of impaired cerebrovascular reactivity.<sup>1,3</sup> Numerous observational studies have linked persistently positive PRx values with poor global outcome in TBI, with well-defined critical thresholds associated with morbidity and mortality.<sup>4,5</sup> Further, PRx is one of only a few continuous indices of cerebrovascular reactivity to have been validated for assessing the

lower limit of autoregulation in an experimental model.<sup>6</sup> Finally, current applications of continuously updating indices of cerebrovascular reactivity have focused on the derivation of “personalized” cerebral perfusion pressure (CPP) targets (also referred to as CPP optimum), utilizing PRx.<sup>7,8</sup> However, the requirement of invasive ICP measurements for PRx calculation is a limitation of the technique.

Various other continuous indices of cerebrovascular reactivity exist based on other invasive and non-invasive monitoring devices employed after TBI.<sup>3,9</sup> In particular, non-invasive transcranial Doppler (TCD) can be utilized to derive flow-based indices.<sup>4,10</sup> Recent multivariate covariance analysis has confirmed a close association between non-invasive TCD derived systolic flow index (Sx\_a): the moving correlation between systolic flow velocity

Divisions of <sup>1</sup>Anaesthesia and <sup>4</sup>Neurosurgery, Department of Clinical Neurosciences, Addenbrooke’s Hospital, University of Cambridge, Cambridge, United Kingdom.

<sup>2</sup>Department of Surgery and <sup>3</sup>Clinician Investigator Program, Rady Faculty of Health Sciences, University of Manitoba, Winnipeg, Manitoba, Canada.

<sup>5</sup>Institute of Electronic Systems, Warsaw University of Technology, Warsaw, Poland.

(FVs) and MAP and invasively derived ICP based indices, including PRx.<sup>11,12</sup> Further, time series linear modeling techniques highlight this strong relationship between PRx and Sx\_a, while providing evidence to support the ability to estimate PRx accurately using this non-invasive TCD index.<sup>13</sup>

The next natural step would be to attempt the prediction of PRx using this non-invasive TCD measure. This has never been attempted before, given complexity of analysis and limitations surrounding acquisition of continuous longer uninterrupted TCD recordings. The goal of this study was to outline the first experience at predicting PRx using non-invasive Sx\_a, derived from extended duration robotic TCD recordings.

## Methods

### Patient population

The data utilized in this retrospective analysis was part of a prospective observational study conducted over a 6 month period in our the Neurosciences Critical Care Unit (NCCU) at Addenbrooke's Hospital, Cambridge (December 2017 – May 2018). All patients had sustained a moderate to severe TBI and were admitted to the Neurosciences Critical Care Unit (NCCU) at Addenbrooke's Hospital, Cambridge. Patients were intubated and sedated given the severity of their TBI. Invasive ICP monitoring was conducted in accordance with the Brain Trauma Foundation (BTF) guidelines. Therapeutic measures were directed at maintaining ICP <20 mm Hg and CPP >60 mm Hg (datum at the tragus).

TCD monitoring is a part of standard intermittent cerebral monitoring in the NCCU. The application of the newer robotic TCD device (see subsequent description) was therefore in alignment with our usual care, negating the need for formal direct or proxy consent. All data related to patient admission demographics and high frequency digital signals from monitoring devices were collected in an entirely anonymous format. Ethical approval for research using anonymous data acquired as part of clinical practice is not required under United Kingdom regulations.

### Signal acquisition

Various signals were obtained through a combination of invasive and non-invasive methods. Arterial blood pressure (ABP) was obtained through either radial or femoral arterial lines connected to pressure transducers (Baxter Healthcare Corp. CardioVascular Group, Irvine, CA). ICP was acquired via an intraparenchymal strain gauge probe (Codman ICP MicroSensor; Codman & Shurtleff Inc., Raynham, MA). Finally, TCD assessment of middle cerebral artery cerebral blood flow velocity (MCA CBFV) was conducted via a robotic TCD system, the **Delica EMS 9D** (Delica, Shenzhen, China, [www.delicasz.com](http://www.delicasz.com)). This system allows for continuous extended duration recording of MCA CBFV, using robotically controlled TCD probes, with automated correction algorithms for probe shift. To our knowledge, this is the first study on the application of extended duration TCD acquisition via a robotic system in critically ill TBI patients.

This study aimed to record 3–4 h of continuous data from all devices simultaneously, given the previous work from our group on inter-index relationships focused on recording durations of only 0.5–1 h duration because of the limitation of conventional TCD. As such, this data set also proved to be ideal for complex time series modeling and analysis. Only patients with three or more continuous, uninterrupted, ICP and TCD recordings were utilized for this study. Thus, only a subpopulation of the group from the original study were utilized for this analysis. Figure 1 displays an example of the recording setup, including triple bolt, near infrared spectroscopy and robotic TCD.

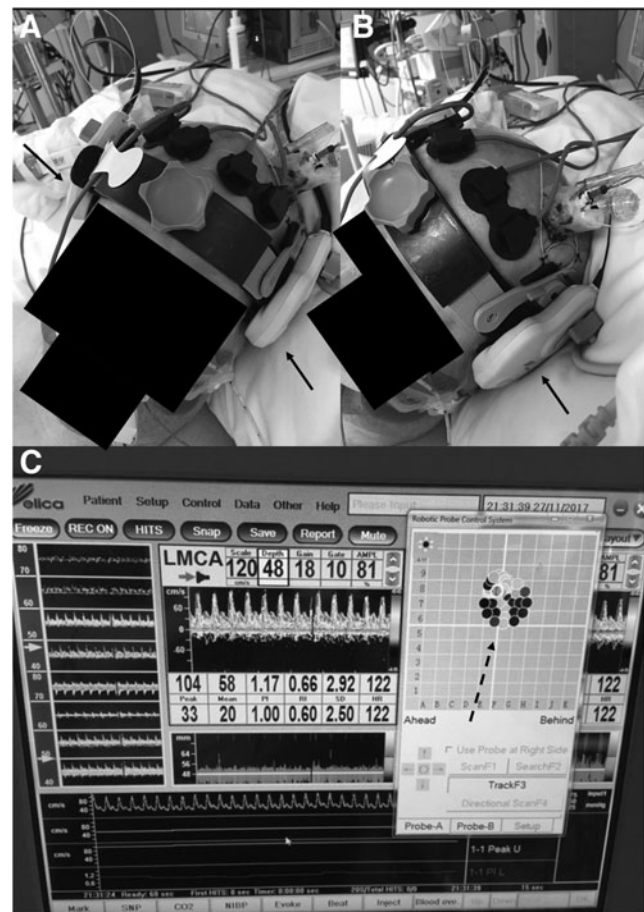


**FIG. 1.** Example of recording setup for ICP, NIRS, and robotic TCD. (A) Left front bolt for ICP monitor, bifrontal NIRS pads (black bi-lobed pads on forehead), and robotic TCD secured with headband (black arrows denote the robotic drives that control TCD probe). (B) Same as A but from the side. (C) Delica EMS 9D TCD program display, showing TCD cerebral blood flow velocity wave form, M-mode display, and automatic correction system (black hashed arrow indicates the automated search pattern for the TCD correction algorithm, insonating at multiple sites, finding the area with superior signal quality). ICP, intracranial pressure; NIRS, near infrared spectroscopy; TCD, transcranial Doppler.

### Signal processing

Signals were recorded using digital data transfer, sampled at frequency of 100 Hz or higher (depending on the modality), using **ICM+ software** (Cambridge Enterprise Ltd, Cambridge, UK, <http://icmplus.neurosurg.cam.ac.uk>). Signal artifacts were removed using a combination of manual and semiautomated methods within ICM+ prior to further processing or analysis.

Post-acquisition processing of the abovementioned signals was conducted using ICM+ software. CPP was determined using the formula:  $CPP = MAP - ICP$ . TCD signal was analyzed from the right side in the majority of the patients, given the right frontal placement of ICP monitors. The only exception to this was when we were unable to obtain quality TCD on the right because of poor windows for TCD.

Systolic flow velocity (FVs) was determined by calculating the maximum flow velocity (FV) over a 1.5 sec window, updated every second. Diastolic flow velocity (FVd) was calculated using the minimum FV over a 1.5 sec window, updated every second. Mean flow velocity (FVm) was calculated using average FV over a 10 sec window, updated every 10 sec (i.e., without data overlap).

Ten second moving averages (updated every 10 sec to avoid data overlap) were calculated for all recorded signals: ICP, ABP (which produced MAP), CPP, FVm, FVs, and FVd. These non-overlapping 10 sec moving average values allowed focus on slow-wave fluctuations in signals by decimating the signal frequency to  $\sim 0.1$  Hz.

Cerebrovascular reactivity indices were derived in a similar fashion across modalities. For PRx, a moving Pearson correlation coefficient was calculated between ICP and MAP using 30 consecutive 10 sec windows (i.e., 5 min of data), updated every minute. Similar to our previous work on non-invasive estimation of PRx using Doppler measures, two non-invasive TCD based indices were also derived: Mx-a (the correlation between FVm and MAP) and Sx-a (the correlation between FVs and MAP). Diastolic flow index (Dx-a) was not evaluated in this study, given our previous work documenting poor time series and linear mixed effects (LME) model performance in relation to PRx.<sup>13</sup>

Data for this analysis were provided in the form of minute by minute time trends of the parameters of interest for each patient. These were extracted from ICM+ into comma separated values (CSV) data sets, which were collated into one continuous data sheet (compiled from all patients).

### Statistical analysis

Similar statistical modeling approach as seen in our previous work for time series data and LME model creation were followed with this data set, and almost identical statistical description to his work will be found subsequently in this article.<sup>13</sup> Minute-by-minute time series data were utilized for the entirety of the analysis that will be described. Statistical significance was set at  $\alpha < 0.05$ . All statistical analysis was conducted using R statistical software (R Core Team [2016]. *R: A Language and Environment for Statistical Computing*. R Foundation for Statistical Computing, Vienna, Austria. URL <https://www.R-project.org/>). The following packages were utilized during the analysis: *tseries*, *forecast*, *lubridate* and *lme4*.

The statistical methods sections to follow will outline the techniques employed to: (1) estimate the autocorrelative structure of PRx in time series, (2) create an accurate model estimating PRx using non-invasive TCD indices of cerebrovascular reactivity via application of LME modeling (with embedded PRx autocorrelative error structure), (3) assess the correlation and agreement between model based estimated PRx and the observed PRx value, and (4) predict PRx using the derived LME models and estimated PRx time series data. For LME model creation/training we utilized the first 80% of the data for each patient, with the remaining 20% utilized for the prediction of PRx using the LME models.

**Autocorrelative structure of PRx.** Prior to being able to model PRx using TCD-based indices, it was necessary to determine the autocorrelation structure of PRx. We used the Box-Jenkins autoregressive integrative moving average (ARIMA) modeling PRx to determine: the autoregressive structure of order “ $p$ ,” the differencing factor or order “ $d$ ,” and the moving average component of order “ $q$ ”; commonly denoted “(p,d,q).” The autoregressive structure refers to the dependence of PRx at time  $t$  (denoted PRx <sub>$t$</sub> ) on previous measures of PRx (i.e., called “lags”), for example, at time  $t-1$  (i.e., PRx <sub>$t-1$</sub>  to, for example, PRx <sub>$t-p$</sub> ), with the order “ $p$ ” indicating how many previous PRx measures PRx <sub>$t$</sub>  is dependent on. Stationarity is defined here as the presence of a stable variance, autocorrelative structure, and mean over time. Stationarity can be introduced by differencing previous PRx measures from current measures, thus removing trending structure from a time series, and allowing further modeling to occur. The differencing order “ $d$ ” refers to how many previous terms should be included in the differencing process. Finally, the moving average term refers to the need to include the error in the ARIMA model at time  $t$  (i.e.,  $\varepsilon_t$ ) as well as “ $q$ ” previous error terms (i.e.,  $\varepsilon_{t-i}$ ,  $i = 1..q$ ).

Assuming stationarity (i.e., no “ $d$ ” order), the ARIMA model folds to a general ARMA model that can be represented by the following formula:

$$PRx_t = c + \varepsilon_t + \sum_{i=1}^p \phi PRx_{t-i} + \sum_{i=1}^q \theta \varepsilon_{t-i}$$

where PRx <sub>$t$</sub>  = PRx at time  $t$ , PRx <sub>$t-i$</sub>  = PRx at time  $t-i$ ,  $\varepsilon_t$  = error at time  $t$ ,  $\varepsilon_{t-i}$  = error at time  $t-i$ ,  $c$  = constant,  $\phi$  and  $\theta$  are parameters at time  $t-i$ ,  $p$  = autoregressive order, and  $q$  = moving average order.

The following process was conducted on all patient recordings, in order to derive the optimal ARIMA structure for the PRx time series. This would provide insight into the approximate best AR-IMA structure for future LME models.

First, data had already been artifact cleared and had a 10 sec moving average filter applied to it, leading to some data smoothing (as described in the signal processing section). Therefore, our initial step for the ARIMA modeling focused on determining stationarity of the signal. This was assessed, and confirmed, using three methods. First, we assessed the autocorrelation function (ACF) correlogram for PRx, looking for a rapid decline in significant lags, indicating a stationary signal. Second, we employed the Augmented Dickey-Fuller (ADF) test to assess for stationarity. Third, we attempted seasonal decomposition using the like-named function in R for each PRx time series, which employs locally weighted scatterplot smoothing (LOWESS) to identify seasonal and trend components to a time series. All of these processes confirmed stationarity within our patient examples.

Second, the autoregressive structure of PRx was assessed using the ACF correlograms and partial autocorrelation function (PACF) correlograms. ACF correlograms were assessed to see how many previous consecutive terms (i.e., “lags”) PRx might be dependent upon. Similarly, the PACF correlograms were assessed to see how many non-consecutive previous lags PRx may be dependent on. Significant level of ACF/PACF correlograms is set at a correlation level of  $\pm(2/N^{1/2})$ , where  $N$  = sample size. We then ran sequential ARMA models for PRx by varying the order “ $p$ ” from 0 to 3, while also varying the moving average order “ $q$ ” from 0 to 3. Given that our analysis for stationarity confirmed a stationary signal within our 10 patient examples, we fixed the differencing order “ $d$ ” at 0. In doing so, we generated 16 separate ARMA models for PRx within each patient. Model superiority was assessed by Akaike Information Criterion (AIC) and log-likelihood (LL), with the lowest AIC and the highest LL indicating the best ARMA model for PRx. In addition, model superiority was assessed via residuals, model ACF and PACF correlograms, with an adequate model represented by random residuals, and ACF/PACF failing to display any lags reaching significance.

**LME modeling of PRx using TCD-derived indices.** LME modeling was conducted on the entire patient population. LME modeling involved various fixed linear models, and a random component introduced into the intercept and independent variable coefficient (based on individual patients). We embedded the PRx ARIMA structure within the LME models (based on the ARIMA modeling results analysis described). This analysis was performed on the full data set, deriving LME models for each patient as well as for the entire population. The following LME models were assessed, initially with random intercept only (stratified by patient), as described: PRx  $\sim$  Sx\_a, PRx  $\sim$  Mx\_a, and PRx  $\sim$  Sx\_a + Mx\_a. All models were corrected using maximum likelihood estimation method. Adequacy of the LME model was assessed via QQ plots and the residuals distribution plot, with linear shape to the QQ plots and normally distributed residuals confirming the validity of the model.

Models were compared using AIC, Bayesian Information Criterion (BIC), LL, and analysis of variance (ANOVA) testing. Superior models were attributed to the lowest AIC, lowest BIC, and

highest LL. Significance differences between models were assessed by ANOVA testing, with a threshold for significance set at  $p < 0.05$ . The top two superior LME models were reported in detail, with a final assessment of model adequacy through ACF/PACF plots of the model residuals, observing for a minimal number of significant lags that decay rapidly.

Generalized fixed-effects models were also created based on the top two LME models. However, these models performed poorly, with substantially inferior AIC, BIC, and LL values. In addition, these general fixed-effects models maintained continuous significant lags in the residuals, further indicating poor modeling of PRx. Hence, these models will not be discussed further.

**Observed versus estimated PRx.** We assessed the correlation between the observed (minute-by-minute) PRx values in our population versus those estimated from our optimal two LME models using Pearson correlation coefficient. We then produced linear regression plots between observed and estimated PRx for the best two LME models, using grand mean data (i.e., mean value per patient). Finally, Bland–Altman plots were produced to assess agreement between the observed and estimated PRx values, using grand mean Fisher transformed data (i.e., Fisher transform applied to both observed and estimated PRx).

**Predicting PRx.** We predicted PRx based on the top two LME models from the previously discussed methods. Using the LME models themselves and the remaining 20% patient data not used in LME model creation, we derived predicted PRx (pPRx) values from observed Sx-a and Mx-a values within this data subset. The predicted values were then compared with the actual observed PRx values during this period using Pearson correlation, linear modeling, and Bland–Altman analysis.

## Results

### Patient demographics

A total of 10 patients with moderate/severe TBI had sufficient quality TCD signals (i.e., at least 3–4 h duration and uninterrupted). The mean age for this population was  $34.5 \pm 17.0$  years, with eight patients being male. The median admission GCS was 7 (interquartile range [IQR] 4–8), with a median admission Glasgow Motor Scale (GCS) motor score of 4 (IQR 2 to 5). The mean duration of ICP/TCD recording was  $223.2 \pm 38.4$  min. Only 80% of the total recording duration for each patient was utilized for model

formation and training, with the remaining 20% reserved for predictive testing.

### Building the model to estimate PRx: ARIMA modeling of PRx

In all 10 patients, the ARIMA structure of PRx was investigated in order to determine the appropriate structure for future LME modeling of the entire population. Upon inspection of the ACF/PACF plots, ADF test results, and seasonal decomposition techniques, it was determined that no significant trend or seasonality was present in any of the 10 patient recordings. Therefore, no differencing order “ $d$ ” was introduced. Next, sequential ARMA models were produced for each patient, varying the autoregressive order “ $p$ ” and moving average order “ $q$ ” from 0 to 3. Across all patients the optimal ARMA model for PRx was found to be (2,0,2), based on the principle of parsimony, and the lowest AIC and highest LL. Figure 2 displays the ACF and PACF plots of PRx for one patient with 4 h of continuous recording, demonstrating a rapid decay in significant lags (implying stationarity). Figure 3 shows the residuals for the ARMA model for PRx in the same patient, with an ARMA structure of (2,0,2). This figure demonstrates a lack of significant lags on ACF and PACF plots, with randomly distributed residuals, confirming the adequacy of the chosen model.

### Model development and accuracy assessment

**LME modeling of PRx using TCD indices.** Using the (2,0,2) PRx ARMA structure identified within the individual patients, various LME models were produced, embedding the PRx ARMA structure within them. Table 1 displays the model characteristics for those LME models derived from Sx\_a and Mx\_a, introducing random effects by patient into the intercept and coefficients. Model superiority was confirmed via ANOVA testing, with the lowest AIC/BIC and highest LL indicating superiority. The top two LME models were:  $PRx \sim Sx\_a$  (AIC = -1564.957, BIC = -1510.159, LL = 792.4786) and  $PRx \sim Sx\_a + Mx\_a$  (AIC = -1597.345, BIC = -1520.627, LL = 812.6726), with random effects by patient introduced into both the coefficients and intercept. The QQ and residual density plots for these top two LME models can be seen in Supplementary Appendix A, displaying normally distributed residuals, indicating model adequacy (see online supplementary material at <http://www.liebertpub.com>). The ACF and PACF

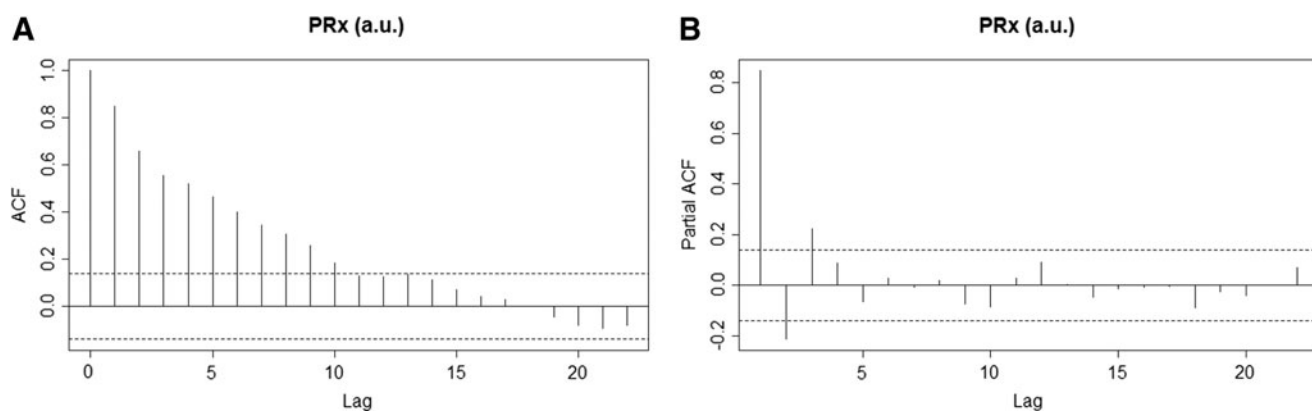


**FIG. 2.** ACF and PACF for PRx: patient example. (A) ACF plot displaying a rapid decay of significant PRx lag, suggesting stationarity. (B) PACF plot, also displaying rapid decay of significant PRx lags. ACF, autocorrelation function; a.u., arbitrary units; PACF, partial autocorrelation function; PRx, pressure reactivity index (correlation between intracranial pressure and mean arterial pressure).

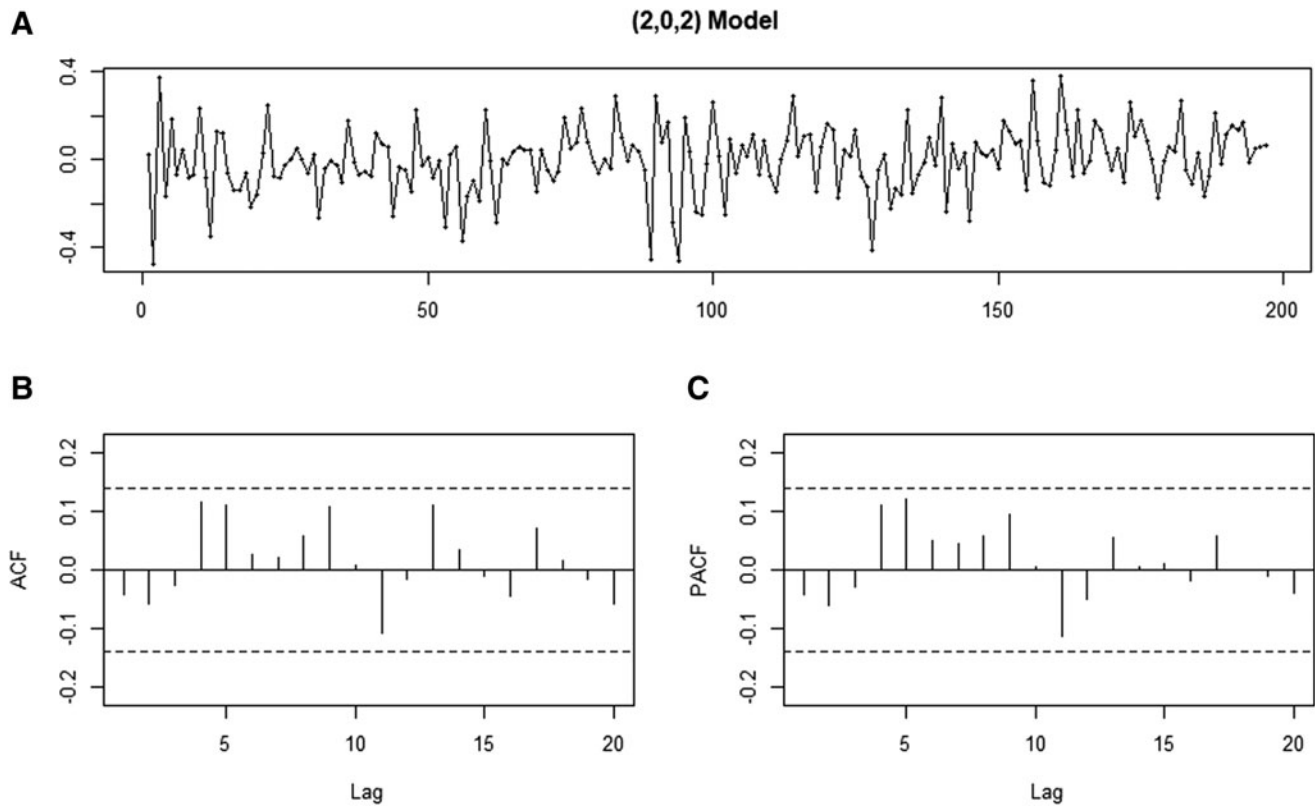


**FIG. 3.** Residual plots for PRx (2,0,2) ARIMA model and their ACF and PACF: a patient example. **(A)** Residual plot for the ARIMA model in this patient example. **(B)** ACF plot displaying no significant lags with (2,0,2) ARIMA model for PRx. **(C)** PACF plot, also no significant lags with (2,0,2) ARIMA model for PRx. ACF, autocorrelation function; ARIMA, autoregressive integrative moving average; PACF, partial autocorrelation function; PRx, pressure reactivity index (correlation between intracranial pressure and mean arterial pressure).

plots for these two models can also be found in Supplementary Appendix A, displaying acceptable rapid decay of significant lags.

Population-based estimation of PRx using Sx-a and Mx-a. Using the top two LME models just described, PRx was estimated using the available Sx\_a and Mx\_a measures in the training data set. Grand mean values were calculated per patient and plotted against the observed PRx values from the data. A strong linear

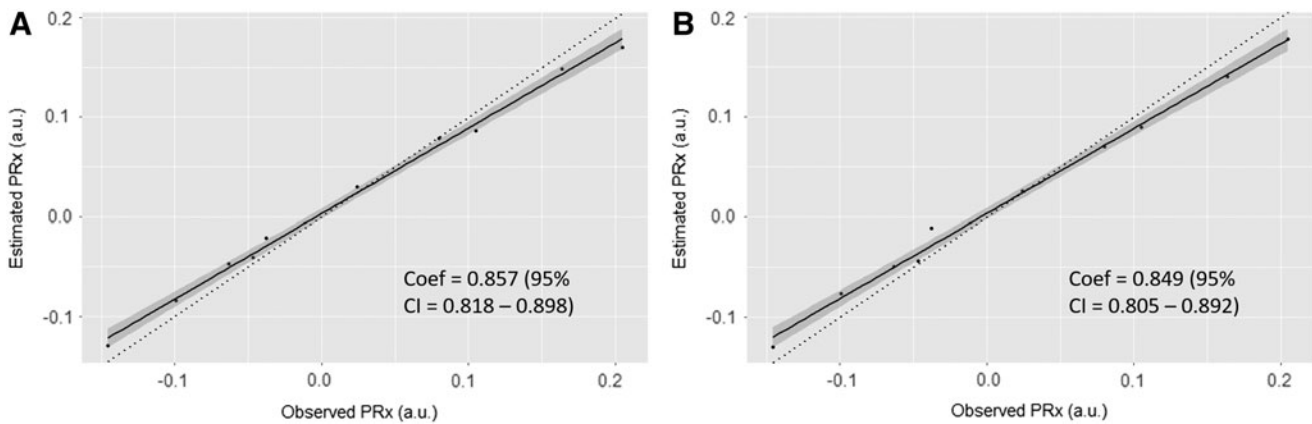
relationship was seen between estimated and observed PRx using both LME models. Figure 4 displays estimated versus observed PRx plots for each model. The PRx ~ Sx\_a model displayed a correlation between estimated and observed values of 0.998 (95% CI=0.990–0.999;  $p < 0.0001$ ), while the PRx ~ Sx\_a + Mx\_a model had a correlation between estimated and observed PRx values of 0.997 (95% CI=0.988–0.999;  $p < 0.0001$ ). Bland–Altman analysis on Fisher transformed results displayed acceptable

TABLE 1. LME MODELS WITH PRx (2,0,2) ARIMA STRUCTURE: ENTIRE POPULATION

LME Model	Fixed effects	Random effects	PRx ARIMA structure				
			<i>p</i>	<i>q</i>	AIC	BIC	LL
PRx ~ Sx_a		Intercept	2	2	−1543.672	−1499.833	779.8362
PRx ~ Mx_a		Intercept	2	2	−1502.348	−1458.509	759.1738
PRx ~ Sx_a + Mx_a		Intercept	2	2	−1550.704	−1501.385	784.3520
<b>PRx ~ Sx_a</b>		<b>Intercept + Sx_a</b>	<b>2</b>	<b>2</b>	<b>−1564.957</b>	<b>−1510.159</b>	<b>792.4768</b>
PRx ~ Mx_a		Intercept + Mx_a	2	2	−1516.367	−1461.569	768.1836
<b>PRx ~ Sx_a + Mx_a</b>		<b>Intercept + Sx_a + Mx_a</b>	<b>2</b>	<b>2</b>	<b>−1597.345</b>	<b>−1520.627</b>	<b>812.6726</b>

Bolded value represents the most appropriate ARIMA structure and LME model for the patient population tested, based on principle of parsimony, lowest AIC, and BIC. There was no integrative parameter (i.e., “d” parameter) included within the ARIMA models, given stationarity testing during patient examples. See Supplementary Appendix A (see online supplementary material at <http://www.liebertpub.com>) and Methods section of manuscript.

AIC, Akaike Information Criterion; ARIMA, autoregressive integrative moving average; BIC, Bayesian Information Criterion; FVs, TCD-based systolic flow velocity; ICP, intracranial pressure; LL, log likelihood, LME, linear mixed-effects model, Mx\_a, mean flow index; *p*, autoregression parameter for ARIMA model; MAP, mean arterial pressure, PRx, pressure reactivity index (correlation between ICP and MAP); *q*, moving average parameter for ARIMA model; Sx\_a, systolic flow index (correlation between TCD based FVs and MAP); TCD, transcranial Doppler.



**FIG. 4.** Linear regression between observed and estimated PRx using estimated PRx from two best LME models. **(A)** LME model:  $PRx \sim Sx\_a$  (random effects with intercept and  $Sx\_a$ ). **(B)** LME model,  $PRx \sim Sx\_a + Mx\_a$  (random effects with intercept,  $Sx\_a$  and  $Mx\_a$ ). Coef, coefficients, form linear model between observed PRx and model estimated PRx. Dotted straight line represents the relationship “ $y=x$ ”, for comparison to our two models. a.u., arbitrary units; ICP, intracranial pressure; LME, linear mixed effects; MAP, mean arterial pressure; PRx, pressure reactivity index (correlation between ICP and MAP).

agreement, with slight underestimation bias in the estimated PRx for both models. This bias in the Bland–Altman plots was seen in our previous work as well.<sup>13</sup> Supplementary Appendix B contains the results of the Bland–Altman analysis comparing the estimated to observed PRx for both LME models (see online supplementary material at <http://www.liebertpub.com>).

#### Predicting PRx using non-invasive TCD parameters

Using the top two LME models just derived, we proceeded to predict PRx (pPRx) using the 20% of data not used in model construction/training. Each patient had 20% of their recording data excluded from the prior model formation/training, each with ICP and TCD derived variables, amounting to ~30–60 min of minute-by-minute data per patient. For each LME model, the  $Sx\_a$  and  $Mx\_a$  values from this new data were entered into the models to derive pPRx. Grand mean values were then calculated per patient. For the model  $PRx \sim Sx\_a$ , the correlation between predicted and observed PRx values was 0.797 (95% CI=0.336–0.949;  $p=0.006$ ). Similarly, for the model  $PRx \sim Sx\_a + Mx\_a$ , the correlation

between predicted and observed PRx was 0.763 (95% CI=0.258–0.941;  $p=0.011$ ). Predicted and observed PRx values displayed a linear association, although not 1:1. Figure 5 displays the predicted versus observed PRx plots for the top two LME models. Bland–Altman analysis of Fisher transformed data demonstrated acceptable agreement between predicted and observed PRx values, with similar underestimation of the predicted PRx values as seen in the training data previously. All Bland–Altman results for comparing pPRx to observed PRx can be found in Supplementary Appendix C (see online supplementary material at <http://www.liebertpub.com>).

#### Discussion

Through the application of time-series ARMA and LME modeling in this pilot study, we have been able to describe, for the first time, the prediction of pressure reactivity index PRx using non-invasive TCD-derived cerebral autoregulation measures (in this case  $Sx\_a$  and  $Mx\_a$ ). Some important aspects of this preliminary pilot work require highlighting.

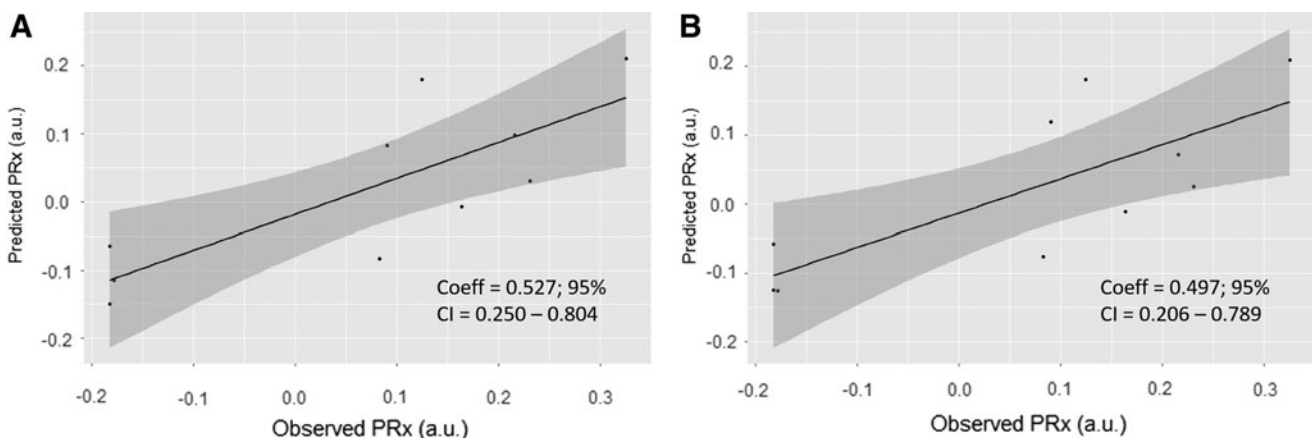


**FIG. 5.** Linear regression between observed and predicted PRx using predicted PRx from two best LME models. **(A)** LME model:  $PRx \sim Sx\_a$  (random effects with intercept and  $Sx\_a$ ). **(B)** LME model:  $PRx \sim Sx\_a + Mx\_a$  (random effects with intercept,  $Sx\_a$  and  $Mx\_a$ ). Coef, coefficients, form linear model between observed PRx and model estimated PRx; a.u., arbitrary units; ICP, intracranial pressure; LME, linear mixed effects; MAP, mean arterial pressure, PRx, pressure reactivity index (correlation between ICP and MAP).

First, through the application of ARMA modeling of PR<sub>x</sub>, and LME modeling of PR<sub>x</sub> using TCD measures, in this unique cohort of patients with extended duration continuous TCD recordings, we have been able to produce LME models that accurately estimate observed PR<sub>x</sub>. This is similar to our prior retrospective work in a large TBI population with TCD.<sup>13</sup> Further, the superior two models from this current cohort were of similar AMRA and mixed-effects structure to those discovered in the prior work, as confirmed through the principle of parsimony. This provides some validation of the previous work, and also provides some evidence to support these models regardless of the duration of TCD recording analyzed. In addition, the bias on Bland–Altman analysis comparing observed to estimated PR<sub>x</sub> displayed the same underestimation bias seen in our previous work, with acceptable agreement.

Second, as with our previous work,<sup>13</sup> the general fixed-effects versions of our top two models performed poorly in estimating PR<sub>x</sub>, with continuous significant autocorrelation in the model residuals. As mentioned in the Methods section, these models were subsequently not reported further. This again confirms patient-by-patient heterogeneity, limiting the extrapolation of this work to other general TBI populations.

Third, the current, and previous,<sup>13</sup> ARMA works demonstrate the strong relationship between measures of CBV (i.e., ICP or PR<sub>x</sub>) and CBF (i.e., CBFV or S<sub>x\_a</sub>/M<sub>x\_a</sub>). This strong association between measures of CBV and CBF is important to emphasize. PR<sub>x</sub>, believed to be a measure of cerebrovascular pressure reactivity, relies on the correlation between vasogenic slow-wave fluctuations in ICP and MAP. ICP in this instance is considered to be a surrogate measure of pulsatile CBV. Thus, PR<sub>x</sub> is measuring changes in CBV in response to changes in MAP, with the corresponding correlation representing cerebral pressure autoregulation and having been validated to measure the lower limit of autoregulation in various experimental models,<sup>6,14,15</sup> whereas the TCD-based cerebrovascular reactivity indices (i.e., S<sub>x\_a</sub> and M<sub>x\_a</sub>) are based on the correlation between slow-wave fluctuations in CBFV and MAP. Thus, TCD-based indices may be considered to be closer measures of flow than those based on non-CBF/CBFV measures. The main limiting factor for TCD measures is the labor-intensive nature inherent in classic TCD devices leading to short and interrupted recordings. Therefore, the application of TCD for regular continuous monitoring of cerebrovascular reactivity has been limited, with no experimental studies in existence validating them as measures of actual pressure autoregulation. Through demonstrating the strong link between PR<sub>x</sub> and S<sub>x\_a</sub>/M<sub>x\_a</sub>, we have demonstrated that TCD-based flow measures are close in relation to the validated pressure autoregulation measure PR<sub>x</sub>. However, it also must be acknowledged that this relationship between volume and flow is not necessarily the same across all patients, as is exemplified by the poor performance of general fixed-effects models and the need for LME modeling demonstrating clearly that the flow/volume relationship varies from patient to patient.

Fourth, we demonstrated for the first time in the literature the ability to predict PR<sub>x</sub> using non-invasive TCD surrogates. Comparing pPR<sub>x</sub> to the observed PR<sub>x</sub> values in the top two models, the correlation is of moderate strength, with a linear relationship between the two and acceptable agreement on Bland–Altman analysis. However, a similar underestimation bias for pPR<sub>x</sub> is present on Bland–Altman analysis. Further, the relationship between pPR<sub>x</sub> and the observed PR<sub>x</sub> was not 1:1, indicating that the prediction is not perfect. This is despite having very strong correlations between the estimated PR<sub>x</sub> and observed PR<sub>x</sub> during the model training phase. This potentially suggests model over fitting during the

training, although it must be acknowledged the current work is mainly a proof of concept and pilot analysis. Much further work is required to optimize the prediction models.

Fifth, for the first time in the literature, we successfully applied the emerging robotic TCD technology for extended duration recording in critically ill TBI patients.

Finally, this work is based on only 10 patients and is entirely preliminary, with results that are not generalizable at this time. Therefore, this type of modeling and prediction of PR<sub>x</sub> should not be conducted outside of a research setting. Much further work is required for validation.

### Limitations

As with our previous work in this area, the patient population was heterogeneous in terms of age, intracranial injury patterns, and therapies directed at ICP/ICP goals. These heterogeneities could impact signal fluctuations and the results obtained for the time series modeling conducted, although in comparison with our larger time series work in TBI, the results of the modeling within this preliminary pilot study were similar, as described.

Second, our patient numbers were small; there were only 10. For the purpose of this type of analysis, we chose only to look at patients with 3–4 h of completely uninterrupted ICP and TCD recordings and, therefore, the data set, although small, is of exceptional size for routine clinical recordings. The requirement for interrupted continuous TCD is a significant limitation with the described modeling, as conventional TCD is currently heavily limited by artifact and signal loss. The application of the robotic TCD mitigated this in our study; however, this technology is relatively new and not without its own limitations, including patient eligibility (i.e., no decompressive craniectomy, no cervical spine immobilization devices), because of the robotic probe's relatively bulky design. Further, even with the application of robotic TCD, it remains difficult to obtain continuous extended-duration recordings given patient motion, bedside procedures, and transport for routine and emergent neuroimaging. As robotic and automated TCD technology improves, we expect to be able to obtain extended-duration uninterrupted recordings throughout a patient's intensive care unit (ICU) stay. Therefore, even though the current results are limited given patient numbers, they provide the platform for future applications once technology catches up with the demands of this type of modeling/prediction.

Third, the ARIMA structure highlighted for PR<sub>x</sub> and the LME models in this study may not be widely applied outside this population. This was also mentioned in our previous publication on this topic. There exists the potential for patient-specific ARIMA structures, and, therefore, the models described in our studies should not be applied clinically. Further, as mentioned, the general fixed-effects versions of our top two models performed poorly in the estimation of PR<sub>x</sub>, resulting in persistently significant residual lags. This also suggests significant patient-by-patient heterogeneity, negating the extrapolation of these results to other general TBI populations at this time. Further work on PR<sub>x</sub>, among other physiological measures in TBI, is required in larger patient populations in order to determine the exact high frequency time series behavior.

Finally, the statistical methodology employed in this study is quite complex. Therefore, the widespread applicability of these techniques is currently limited. However, with the increasing availability of real-time bedside computing software, such constraints are becoming less important as even mathematically sophisticated models can be handled automatically allowing for a

much more user-friendly application of such techniques. Such functions will automate much of the analysis described in our works on time series, requiring limited user input. This will, it is hoped, bring this type of work to the wider clinical world for future multi-center validation studies.

## Conclusion

Through the application of ARMA and LME modeling, it is possible to estimate PRx using non-invasive TCD measures, such as Sx<sub>a</sub> and Mx<sub>a</sub>. This is the first preliminary attempt at doing so. Further work is required prior to application in a clinical setting, as this current work should be considered experimental at this time.

## Acknowledgments

This work was made possible through salary support through the Cambridge Commonwealth Trust Scholarship, the Royal College of Surgeons of Canada – Harry S. Morton Travelling Fellowship in Surgery, and the University of Manitoba Clinician Investigator Program. These studies were supported by National Institute for Healthcare Research (NIHR, UK) through the Acute Brain Injury and Repair theme of the Cambridge NIHR Biomedical Research Centre and an NIHR Senior Investigator Award to D.K.M. The authors were also supported by a European Union Framework Program 7 grant (CENTER-TBI, Grant Agreement No. 602150).

## Author Disclosure Statement

F.A.Z. has received salary support for dedicated research time, during which this project was partially completed. Such salary support came from: the Cambridge Commonwealth Trust Scholarship, the Royal College of Surgeons of Canada – Harry S. Morton Travelling Fellowship in Surgery, and the University of Manitoba Clinician Investigator Program. P.S. and M.C. have financial interest in a part of licensing fee for ICM+ software (Cambridge Enterprise Ltd, UK). D.K.M. has consultancy agreements and/or research collaborations with GlaxoSmithKline Ltd., Ornim Medical, Shire Medical Ltd., Calico Inc.; Pfizer Ltd., Pressura Ltd., Glide Pharma Ltd., and NeuroTraumaSciences LLC. The other authors have nothing to disclose.

## References

1. Czosnyka, M., Smielewski, P., Kirkpatrick, P., Laing, R.J., Menon, D., and Pickard, J.D. (1997). Continuous assessment of the cerebral vasomotor reactivity in head injury. *Neurosurgery* 41, 11–19.
2. Czosnyka, M., Miller, C., and Participants in the International Multidisciplinary Consensus Conference on Multimodality Monitoring. (2014). Monitoring of cerebral autoregulation. *Neurocrit. Care* 21, Suppl. 2, S95–102.
3. Zeiler, F.A., Donnelly, J., Calviello, L., Smielewski, P., Menon, D.K., and Czosnyka, M. (2017). Pressure autoregulation measurement techniques in adult traumatic brain injury, Part II: A scoping review of continuous methods. *J. Neurotrauma* 34, 3224–3237.
4. Sorrentino, E., Diedler, J., Kasprówicz, M., Budohoski, K.P., Hau-brich, C., Smielewski, P., Outtrim, J.G., Manktelow, A., Hutchinson,

- P.J., Pickard, J.D., Menon, D.K., and Czosnyka, M. (2012). Critical thresholds for cerebrovascular reactivity after traumatic brain injury. *Neurocrit. Care* 16, 258–266.
5. Zeiler, F.A., Donnelly, J., Smielewski, P., Menon, D., Hutchinson, P.J., and Czosnyka, M. (2018). Critical thresholds of ICP derived continuous cerebrovascular reactivity indices for outcome prediction in non-craniectomized TBI patients: PRx, PAX and RAC. *J. Neurotrauma* 160, 1315–1324.
6. Brady, K.M., Lee, J.K., Kibler, K.K., Easley, R.B., Koehler, R.C., and Shaffner, D.H. (2008). Continuous measurement of autoregulation by spontaneous fluctuations in cerebral perfusion pressure: comparison of 3 methods. *Stroke* 39, 2531–2537.
7. Howells, T., Smielewski, P., Donnelly, J., Czosnyka, M., Hutchinson, P.J.A., Menon, D.K., Enblad, P., and Aries, M.J.H. (2018). Optimal cerebral perfusion pressure in centers with different treatment protocols. *Crit. Care Med.* 46, e235–e241.
8. Needham, E., McFadyen, C., Newcombe, V., Synnot, A.J., Czosnyka, M., and Menon, D. (2017). Cerebral perfusion pressure targets individualized to pressure-reactivity index in moderate to severe traumatic brain injury: a systematic review. *J. Neurotrauma* 34, 963–970.
9. Zeiler, F.A., Donnelly, J., Calviello, L., Menon, D.K., Smielewski, P., and Czosnyka, M. (2017). Pressure autoregulation measurement techniques in adult traumatic brain injury, Part I: A scoping review of intermittent/semi-intermittent methods. *J. Neurotrauma* 34, 3207–3223.
10. Budohoski, K.P., Reinhard, M., Aries, M.J.H., Czosnyka, Z., Smielewski, P., Pickard, J.D., Kirkpatrick, P.J., and Czosnyka, M. (2012). Monitoring cerebral autoregulation after head injury. Which component of transcranial Doppler flow velocity is optimal? *Neurocrit. Care* 17, 211–218.
11. Zeiler, F.A., Donnelly, J., Menon, D.K., Smielewski, P., Zweifel, C., Brady, K., and Czosnyka, M. (2017). Continuous autoregulatory indices derived from multi-modal monitoring: each one is not like the other. *J. Neurotrauma* 34, 3070–3080.
12. Zeiler, F.A., Cardim, D., Donnelly, J., Menon, D.K., Czosnyka, M., and Smielewski, P. (2018). Transcranial doppler systolic flow index and ICP-derived cerebrovascular reactivity indices in traumatic brain injury. *J. Neurotrauma* 35, 314–322.
13. Zeiler, F.A., Smielewski, P., Donnelly, J., Czosnyka, M., Menon, D., and Ercole, A. (2018). Estimating pressure reactivity index using non-invasive doppler based systolic flow index. *J. Neurotrauma* 35, 1559–1568.
14. Zeiler, F.A., Lee, J.K., Smielewski, P., Czosnyka, M., and Brady, K. (2018). Validation of ICP derived cerebrovascular reactivity indices against the lower limit of autoregulation, Part II: Experimental model of arterial hypotension. *J. Neurotrauma* [Epub ahead of print; doi: 10.1089/neu.2017.5604].
15. Zeiler, F.A., Donnelly, J., Calviello, L., Lee, J.K., Smielewski, P., Brady, K., Kim, D.J., and Czosnyka, M. (2018). Validation of pressure reactivity and pulse amplitude indices against the lower limit of autoregulation, Part I: Experimental intracranial hypertension. *J. Neurotrauma* [Epub ahead of print; doi: 10.1089/neu.2017.5603].

Address correspondence to:  
*Frederick A. Zeiler, BSc, MD, FRCSC*  
*Department of Surgery*  
*Rady Faculty of Health Sciences*  
*University of Manitoba*  
*Winnipeg, Manitoba*  
*Canada*

E-mail: umzeiler@myumanitoba.ca